Investigation of the anodic behavior of nickel in H_2SO_4 solutions using galvanostatic polarization technique. III. Inhibition of pitting corrosion using nitrogen-containing organic compounds

Arej S. Al-Gorair[a], S. Abd El Wanees[b,c,]*, H. Hawsawi[d], Mahmoud G.A. Saleh[e], M. Abdallah[f,g]

[a]*Chemistry Department, College of Science, Princess Nourah bint Abdulrahman University, Riyadh, Saudi Arabia, email: asalgorir@pnu.edu.sa*
[b]*Chemistry Department, Faculty of Science, Zagazig University, Zagazig, Egypt, email: s_wanees@yahoo.com*
[c]*Faculty College of Umluj, Umluj, Tabuk University, Tabuk, Saudi Arabia*
[d]*University College of Alwajh, Alwajh, Tabuk University, Tabuk, Saudi Arabia, email: hnoho60@gmail.com*
[e]*Chemistry Department, Faculty of Science, Northern Border University, Arar, Saudi Arabia, email: mgsaleh72@yahoo.com*
[f]*Chemistry Department, Faculty of Science, Umm Al-Qura University, Makkah Al Mukaramha, Saudi Arabia, email: metwally555@yahoo.com*
[g]*Chemistry Department, Faculty of Science, Banha University, Banha, Egypt*

ABSTRACT

Thiourea, (Inh I), N-allylthiourea, (Inh II), and 3-allyl-1-[(2-methoxyphenyl)methyl]thiourea (Inh III) were used to mitigate the pitting corrosion of Ni in 0.01 M H_2SO_4 by the galvanostatic polarization technique. The used compounds decrease the pitting corrosion by displacement of the pitting potential, E_{pit} into more positive values, with decreasing the amount of electricity, Q_{inh}, required to reach E_{pit}. The inhibition efficacy, η, was found to increase with raising the inhibitor concentration and depend on its kind. The inhibition efficacy, η, increases in the sequence Inh I < Inh II < Inh III. The inhibitive action of these compounds is discussed in terms of blocking the electrode surface through an adsorption process following the Temkin isotherm. The calculated values of ΔG°_{ads} are found to be –48.63, –50.18, and –51.84 kJ/mol for Inh I, Inh II, and Inh III, successively. These values are compatible with a chemisorption process including the transfer of electrons from the inhibitor molecule to the Ni metal surface.

Keywords: Nickel; Pitting corrosion; Inhibition; Oxide film repair; Passivity; Thiourea derivatives

1. Introduction

Pitting corrosion is one of the most dangerous types of corrosion that occurs for metals and metal alloys. The most dangerous anions Cl^-, ClO_3^-, and ClO_4^- induce the major role in the initiation and propagation of the localized pitting corrosion for most passive metals and stainless steel [1–6]. An important characteristic of pitting corrosion is the fact that pits can nucleate and grow at potentials below the pitting potential [6–12]. Pitting corrosion is characterized by different stages, starting by passive film destruction, metastable pits formation, and pit growth followed by pit propagation ending by metal disintegration [6,10,11].

For facing this type of attack to protect the metal and preserve the mineral wealth from loss, inhibitors should be added to the corrosion environment. Literature

---

* Corresponding author.

indicated that most of the used inhibitors are inorganic anions [4,5,11,12] or organic molecules containing hetero-atoms rich by electron density such as P, O, N, and S in their chemical structures [13–20]. The inhibition influence of such molecules could be related to their adsorption through active centers which are rich in electron density on the corroding metal surface creating an insulating film that prohibits the aggressive ions to reach the metal surface. The kind of adsorption of such molecules relies on different factors such as the nature and the charge of the metal, the kind of corrosive anions, and the chemical structure of organic materials [21].

Nickel is one of the most utilized metals that used in various industrial applications. The pure metal exerts a good corrosion resistance which is frequently due to the formed protective oxide film on its surface [12,14,21]. It is found that the passive film formed on Ni in dilute concentrations of sulfuric acid was composed of mixed Ni oxide films while a hydrated $NiSO_4$ was formed in highly concentrated solutions [21,22]. The study of the corrosion inhibition of Ni in sulfuric acid solutions is important due to the frequently use of Ni in contact with the acidic solutions [23]. The present study aims to evaluate the efficiencies of some N-containing organic compounds such as thiourea and thiourea derivatives. Such molecules are rich in S and N atoms in their structure. Thiourea (Inh I), N-allylthiourea (Inh II), and 3-allyl-1-[(2-methoxyphenyl)methyl]thiourea, Inh (III) are selected as corrosion inhibitors for pitting corrosion of nickel in 0.01 M H_2SO_4 solutions mixed with 0.01 M ClO_4^- ions using the galvanostatic polarization technique.

Due to the increase in the aggressiveness of the sulfate and perchlorate ions on the Ni passivity by temperature [24], the influence of temperature on the initiation and inhibition of pitting corrosion was examined. Some thermodynamic parameters including the activation energies, E_a, enthalpy of activation, ΔH_a, and entropy of activation, ΔS_a are computed and discussed. Also, the adsorption thermodynamic parameters like the standard free energy, $\Delta G°_{ads}$, and the equilibrium constant, K_{ads}, are calculated and explained. Surface examination for some of the corroded nickel samples in the corrosive and inhibitive solutions is examined by scanning electron microscopy (SEM).

2. Experimental techniques

2.1. Materials

Spectroscopically pure Ni electrode (99.999%) was made from spec-pure nickel rod (Johnson-Matthey, U.K.). The electrode was fixed to a borosilicate glass tube with epoxy resin so that the total exposed surface area was 0.97 cm². Electrical contact was achieved through a copper wire soldered to the end of the rod not exposed to the solution. Before being used the electrode was abraded with the finer grades emery papers to mirror finish [6,24]. Before each test, the surface area of the Ni metal was polished by abrading with different grades of finely polished papers. Then, the electrode was cleaned by rinsing with acetone followed by bi-distilled water and the test solution before inundation in the investigated solution. The used inhibitors are thiourea, N-allylthiourea, and 3-allyl-1-[(2-methoxyphenyl) methyl]thiourea, Table 1.
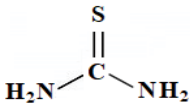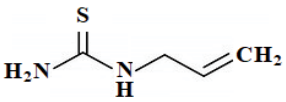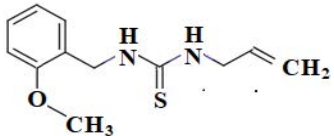
The examined solutions were prepared from A.R. H_2SO_4, $NaClO_4$ (Fluka), and bi-distilled water. Various amounts of inhibitors (1×10^{-6} M to 5×10^{-3} M) are added to 0.01 M H_2SO_4 containing 0.01 M $NaClO_4$. Experiments were done at 25°C, except otherwise carried at various temperatures. To ensure the repeatability of the results, each experiment was triplicated and the data were nearly similar. The SEM, JEOL TM, JSM-T100 (Japan), is employed to examine the surface of some corroded Ni surfaces in 0.01 M H_2SO_4 mixed with 0.01 M $NaClO_4$ without and with 0.0001 M of the different inhibitors.

2.2. Electrolytic cell

The electrolytic cell used for electrochemical experiments was composed of two compartments separated by a fritted glass disc to prevent mixing of anolyte and catholyte [26–28]. The cell has a double-walled jacket through which water at the adjusted temperature was circulated. Three kinds of electrodes are employed (platinum wire as a counter electrode, nickel as a working electrode, and a saturated calomel electrode, SCE, as a reference electrode). The SCE was connected with a Luggin capillary positioned close to the working electrode surface in order to minimize

Table 1
Name, molecular formula, chemical structure, and molecular weight of the utilized inhibitors

Type and name of the inhibitors	Molecular formula	Chemical structure	Molecular weight
Thiourea (Inh I)	CH_4N_2S		76.12 g/mol
N-allylhiourea (Inh II)	$C_4H_8N_2S$		116.19 g/mol
3-Allyl-1-[(2-methoxyph- enyl)methyl]thiourea (Inh III)	$C_{11}H_{14}N_2OS$		222.2 g/mol

ohmic potential drop. Before carrying polarization, the Ni electrode was subjected to cathodic pretreatment for 20 min in the test solution to reduce any overlying oxides film that would be formed on the metal surface before running the experiment. An ultra-thermostat, Polyscience-type (USA) was used for adjusting the reaction temperature. Each test was carried out with a latterly prepared electrode and a neoteric solution. The potential-time curves at a constant applied current were plotted on a recorder unit, Cole Parmer Instruments (USA).

3. Results and discussion

3.1. Effect of inhibitor concentration

Fig. 1 explains the galvanostatic anodic polarization curves of nickel in 0.01 M H_2SO_4 containing 0.01 M $NaClO_4$ solutions without and with various additions of 3-allyl-1-[(2-methoxyphenyl)methyl]-thiourea (Inh III), at 1.0 mA/cm^2 and 25°C. Comparable curves are gained with the addition of N-allylthiourea (Inh II) and thiourea (Inh I), curves not displayed. The data of the curves of Fig. 1 and the likes are recognized by a potential jump (region I) confirming the decay of H_2 over-voltage on the nickel surface subsequent by charging of the electrical double layer [25,29,30]. After the decay step, the potential of the Ni electrode modifies slowly with time to give two potential arrests (zone II) followed by an inclined rise in the potential (zone III), passive region, till reaching the pitting potential, E_{pit}, at which perchlorate ions start to initiate the pitting corrosion [31]. The data of the polarized curves in the presence of 3-allyl-1-[(2-methoxyphenyl)methyl]thiourea are indicated by curves 2–8 in Fig. 1. The regions I and II of curves 2–8 match in similarity that of the inhibitor-free, curve 1. The presence of the inhibitor enhances oxide film repair $(\partial E/\partial t)_i$ during the formation of the passive region, (zone III) with a shift of E_{pit} into the noble direction. This is due to the retardation of the pitting corrosion [6]. The oxidation processes represented by the arrests a and b would confirm the formation of NiO as discussed early [25,32–34], while the rise in the potential values, after the active oxidation process, $(\partial E/\partial t)_{ii}$ could be assigned to the formation of more NiO on the metal surface [25].

However, Fig. 1 depicts that in the case of the inhibitor-free solution, curve 1, the anodic polarized curve indicated that the E_{pit} on the passive region located at 805 mV$_{SCE}$ due to the damage of the oxide film with the initiation of localized pitting corrosion [29,35]. A local active cell is formed with the initiation of pitting corrosion on the oxide film. This attitude is explained early as due to the specific adsorption of the ClO_4^- and Cl^- ions on the passive oxide film with the formation of metastable pits [29,36]. It must be clarified that Cl^- ions are produced from the reduction of ClO_4^- ions by the effect of Ni^{+2} ions at the local active points to initiate the pitting corrosion [37,38]. Little additions of inhibitor delay the pitting corrosion by shifting the E_{pit} into the more positive values. The presence of 1×10^{-6} M of inhibitor III (curve 2, Fig. 1) displaces E_{pit} into 865 mV$_{SCE}$, while the addition of 1×10^{-3} M of inhibitor III (curve 8, Fig. 1) rises E_{pit} into 1,170 mV$_{SCE}$ confirming that inhibitor has delayed the pitting corrosion by displacement of the aggressive ion from the electrode surface. The presence of fluctuations after the breakdown potential, E_{pit}, can be referred to as competition between the corrosive (ClO_4^- and Cl^- ions) and inhibitive species on the oxide film surface. The formed metastable pits stop propagating when the rate of oxide film repair is lightly exceeded that of oxide film destruction, by the effect of organic molecules [35].

The destructive effect of ClO_4^- ions on the Ni sample after the anodization process is depicted in Fig. 2. This figure resembles the scanning electron micrograph (SEM) of the Ni sample after carrying the anodic polarization experiment in 0.01 M H_2SO_4 mixed with 0.01 M ClO_4^- ions. It is noted that the surface of the Ni sample has several irregularly distributed pits surrounded by corrosion products. This confirms the destruction influence by each of Cl^- and ClO_4^- ions for the passive film with a generation of well-defined pits, distributed on the metal surface.
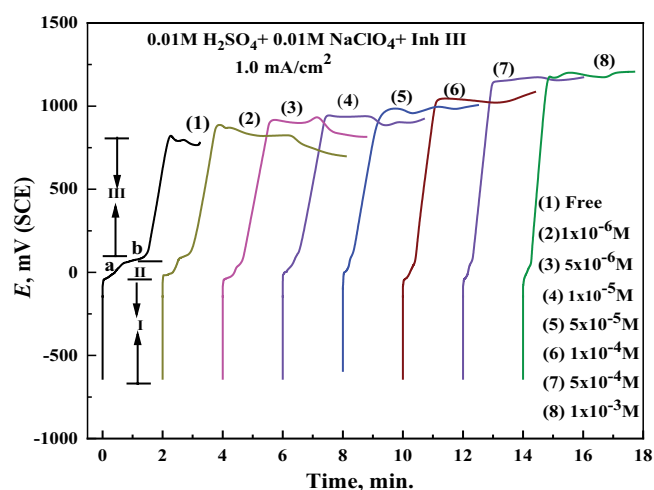

Fig. 1. Galvanostatic anodic polarization curves of Ni in 0.01 M H_2SO_4 mixed with 0.01 M $NaClO_4$ devoid of and containing different amounts of 3-allyl-1-[(2-methoxyphenyl)methyl]thiourea, at 1.0 mA/cm^2 and 25°C.
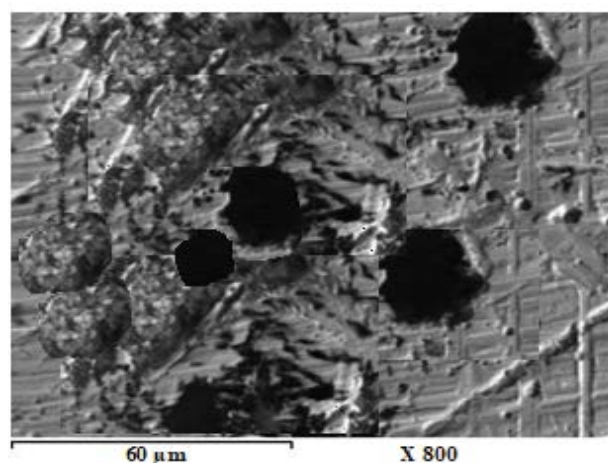

Fig. 2. Scanning electron micrograph (SEM) of the anodically polarized Ni sample in 0.01 M H_2SO_4 mixed with 0.01 M ClO_4^- ions, at 25°C.

The relation between the pitting corrosion potential, E_{pit}, and the logarithmic concentration of the added inhibitor can be represented by plots in Fig. 3. The plots give segmented S-shape curves similar to an adsorption isotherm. It is clear that the pitting potential, E_{pit}, rises gradually with increasing the amount of inhibitor due to the adsorption of the inhibitor molecules on the metal surface preventing the pitting propagation [35].

Fig. 4 depicts the rise in the rate of oxide-film repair, $\partial E/\partial t$, with the log C_{inh} of the added inhibitors. This figure depicts the increase in the $\partial E/\partial t$ values with the added inhibitor, according to the segmented S-shaped curve, which confirms the existence of an adsorption process of the used organic molecules on the passive nickel film [35].

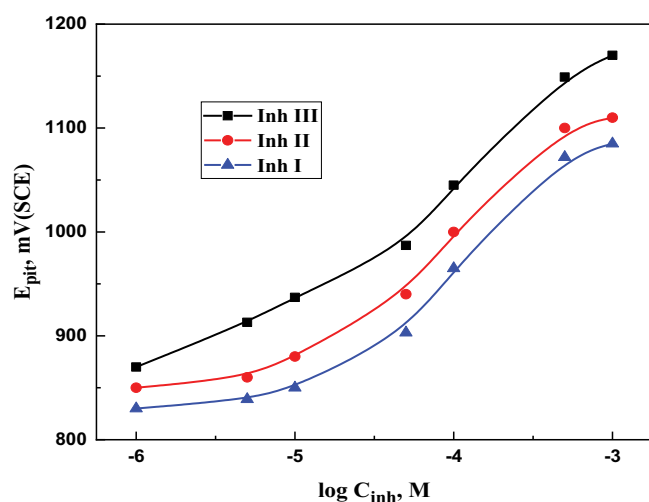Figs. 5A–C illustrate the surface morphology of the Ni sample after an anodic polarization experiment in 0.01 M H_2SO_4 mixed with 0.01 M ClO_4^- ions in the presence of 0.00001 M thiourea, N-allylthiourea, and 3-allyl-1-[(2-methoxyphenyl)methyl]thiourea. It is obvious the existence of some fine pits on the metal surface surrounded by some corrosion products in comparison with thick pits formed in the absence of such inhibitor, Fig. 2. This confirms that the existence of the inhibitor resists the destructive effect of Cl^- and ClO_4^- ions and protects the metal from pitting corrosion.

The values of the inhibition efficacy, η %, can be calculated from the quantity of electricity (in mC cm^{-2} unit) consumed during anodic polarization till the initiation of pitting corrosion and reaching E_{pit} without (Q_{free}) and with inhibitor (Q_{inh}) according to the following equation:

$$\eta = \left(1 - \frac{Q_{inh}}{Q_{free}}\right) \times 100 \tag{1}$$

In the present study, the experimental reproducibility of the inhibition efficiency in a triplicate determination is good (the relative standard deviation values of three parallel experiments were lower than 1.3% as shown in Table 1). The calculated inhibition efficacies values are listed in Table 2. 3-Allyl-1-[(2-methoxyphenyl)methyl] thiourea gives the high inhibition efficacy reaching 68.00% at 1×10^{-3} M concentration. The strength of the added inhibitors towards the retardation of the localized pitting corrosion on Ni in the sulfuric acid solution containing ClO_4^- ions decreases in the order: 3-allyl-1-[(2-methoxyphenyl)methyl]thiourea > N-allylthiourea > thiourea. This order confirms the increased tendency of the employed inhibitors towards the inhibition of the localized pitting corrosion. Thiourea is a less effective inhibitor while 3-allyl-1-[(2-methoxyphenyl)methyl]thiourea followed by N-allylthiourea are a more effective corrosion inhibitor. The inhibition mechanism of the employed inhibitors could be referred to as the competitive adsorption between the organic molecules through the adsorption of the active centers (N and S atoms besides the π-bonds of benzene ring) and the aggressive Cl^- and ClO_4^- ions on the Ni surface which delays the destructive effect of Cl^- and ClO_4^- ions by shifting the E_{pit} into the noble direction retarding the localized pitting corrosion [39]. The adsorbed inhibitors may be combined into the passive film improving the passivity against the destructive effect of ClO_4^- ions [39].

3.2. Adsorption isotherm

Inhibition by organic inhibitors is, primarily, owing to their capability to adsorb onto a corroded metal surface forming an insulating layer. The suitable adsorption isotherm that confirms the adsorption process of the organic molecules on the metal surface is crucial as it supplies important evidence about the nature of metal-inhibitor interaction. Generally, the adsorption of the inhibitor molecules depends on various factors; among these is the type of heteroatoms located in the inhibitor molecule, the nature of substrate metal, and the kind of interaction between the inhibitive molecules and the metal surface [40]. Several adsorption isotherms were tried to fit the data assess the adsorption behavior of the inhibitors including the Temkin, Langmuir,

Fig. 3. Variation of the pitting potential, $E_{pitting}$, with the logarithmic concentration of the inhibitors, log C_{inh}, for Ni in 0.01 M H_2SO_4 mixed with 0.01 M Na_2ClO_4, at 25°C.
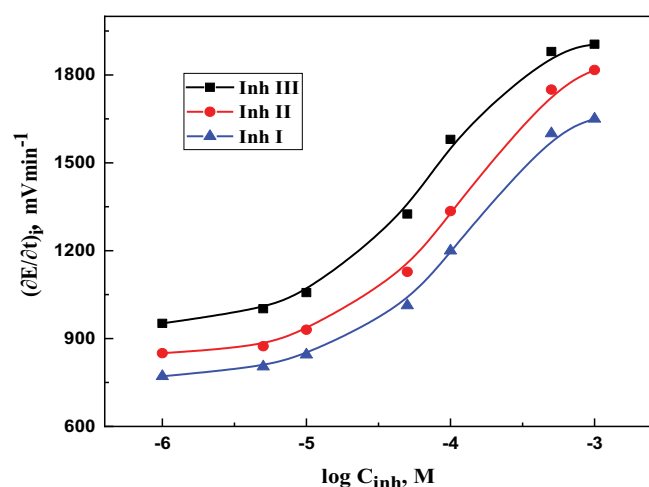

Fig. 4. Variation of the rate of oxide film repair, $(\partial E/\partial t)_i$, with the logarithmic concentration of the inhibitor, C_{inh}, for Ni in 0.01 M H_2SO_4 and 0.01 M $NaClO_4$, at 25°C.
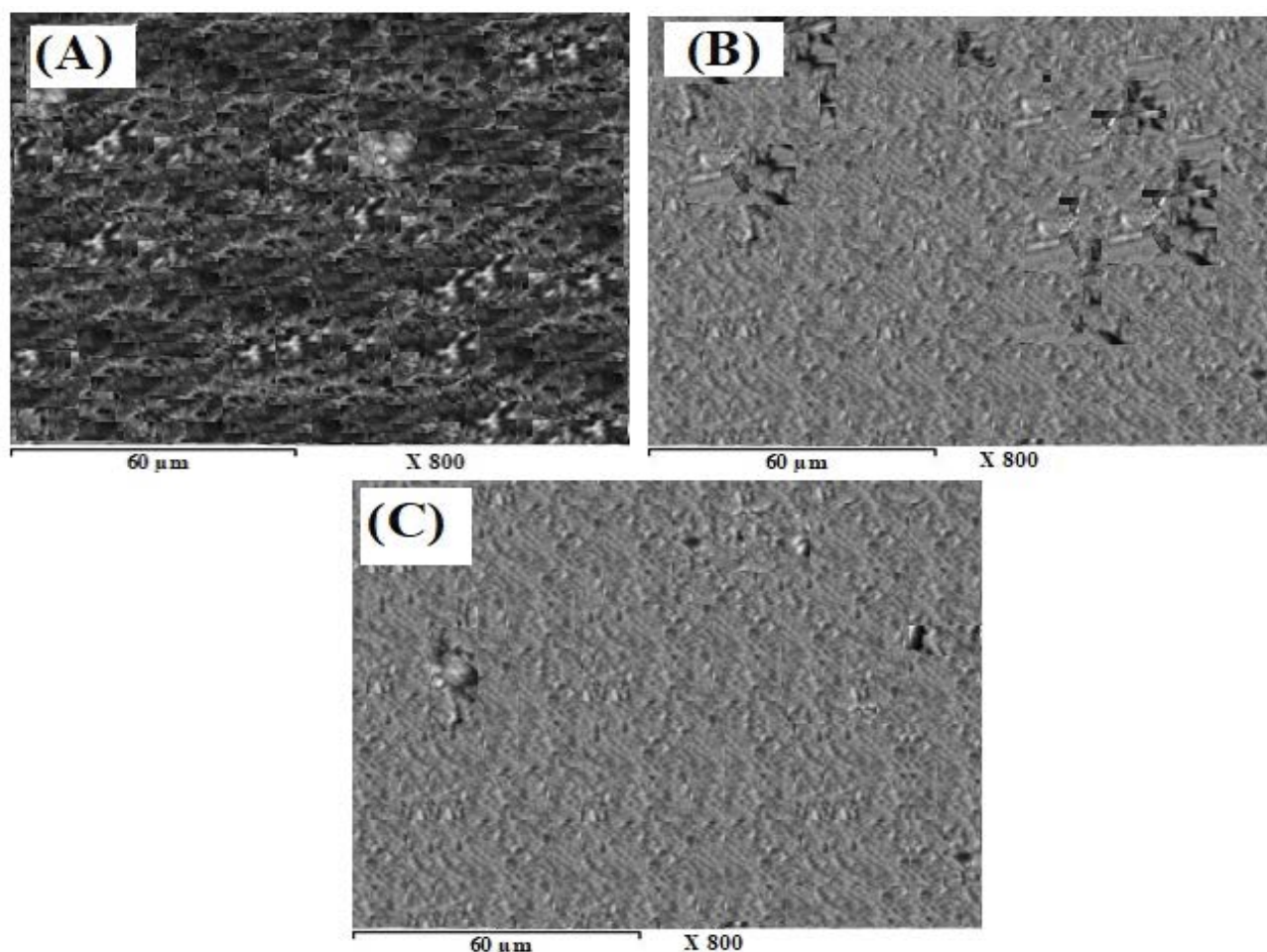
Fig. 5. Scanning electron micrograph (SEM) of the anodically polarized Ni sample in 0.01 M H$_2$SO$_4$ mixed with 0.01 M ClO$_4^-$ ions in the presence of 0.0001 M of (A) thiourea, (B) N-allylthiourea, and (C) 3-allyl-1-[(2-methoxyphenyl)methyl]thiourea, at 25°C.

Table 2
Values of the inhibition efficiency, with relative standard deviation, for inhibitors toward the pitting corrosion of Ni in 0.01 M H$_2$SO$_4$ mixed with 0.01 M NaClO$_4$ solutions at 25°C

Concentration, M	Inhibition efficiency, η %		
	Inh I	Inh II	Inh III
1 × 10^{-6} M	12.0 ± 0.89	14.9 ± 0.77	20.2 ± 1.09
5 × 10^{-6} M	19.8 ± 0.95	26.0 ± 0.95	28.7 ± 0.98
1 × 10^{-5} M	24.7 ± 0.92	29.6 ± 0.88	34.5 ± 0.87
5 × 10^{-5} M	34.9 ± 0.88	39.4 ± 0.93	48.3 ± 0.89
1 × 10^{-4} M	39.4 ± 0.78	44.3 ± 0.94	51.9 ± 0.68
5 × 10^{-4} M	49.6 ± 0.79	54.1 ± 0.86	58.6 ± 0.74
1 × 10^{-3} M	53.2 ± 0.85	59.0 ± 0.94	64.3 ± 0.86

and Frumkin isotherm. Among the three adsorption isotherms, the Temkin adsorption isotherm was found to provide the best fit. In Figs. 6A–C the linearly fit data obtained and the values of the regression coefficient, $R^2 \geq 0.996$) of Fig. 6A confirm the Temkin adsorption isotherm [41,42].

The Temkin adsorption model was preferable to describe the adsorption of such compounds on the metal surface. In all isotherms, the value of θ can be computed from the values of the quantity of electricity consumed from starting the experiment till reaching E_{pit}, Q_{free} (in case of inhibitor-free solution), and Q_{inh} (with inhibitor solution) is using the equation [21]:

$$\theta = \left(1 - \frac{Q_{inh}}{Q_{free}}\right) \qquad (2)$$

According to this type of isotherm the relation between the surface coverage, θ, and the corresponding inhibitor amount, C, can be performed by the relation [41,42]:

$$e^{f\theta} = K_{ads}C \qquad (3)$$

or

$$\theta = \frac{k_{ads}}{f} + \frac{1}{f}\ln C \qquad (4)$$

where K_{ads} represents the adsorption–desorption equilibrium constant while f is the molecular interaction constant. The value of f relies on the intermolecular interaction in the adsorbed film besides the heterogeneity of the metal surface. When f takes positive values means the mutual attraction between molecules, and for negative values of f, repulsion occurs [41]. Typical plots of θ vs. ln$C$ are depicted in Fig. 6. Straight lines are obtained confirming the Temkin adsorption isotherm. The values of K_{ads} and f parameters can be determined from the intercept and slope of Fig. 6, Table 3.

The free energy of adsorption, $\Delta G°_{ads}$, of the different used molecules can be derived from the values of equilibrium constant, K_{ads} using the relation [43]:

$$\Delta G°_{ads} = 2.303RT\log\left(55.5K_{ads}\right) \qquad (5)$$

where R is the gas constant (8.314 J/K/mol), 55.5 is the concentration of H_2O (mol/l) in the investigated solution, and T is the absolute temperature. Various values of $\Delta G°_{ads}$ are represented in Table 3. The obtained values of $\Delta G°_{ads}$ are –48.63,

–50.18, and –51.84 kJ/mol with thiourea, allyl thiourea, and N-allyl-1-[(2-methoxyphenyl)methyl]thiourea, successively. Primarily, $\Delta G°_{ads}$ values up to –20 kJ/mol are harmonious with the physical adsorption, while those more negative than 40 kJ/mol are conjugated with the chemisorption process due to coordinate bond formation by sharing or transfer of electrons from the rich electron centers of the used inhibitor molecules to the metal surface [44]. The calculated values of $\Delta G°_{ads}$ are compatible with a chemisorption

Table 3
Adsorption parameters of the inhibitors (f, K_{ads}, and $\Delta G°_{ads}$) on Ni surface in 0.01 M H_2SO_4 mixed with 0.01 M $NaClO_4$ solutions at 25°C

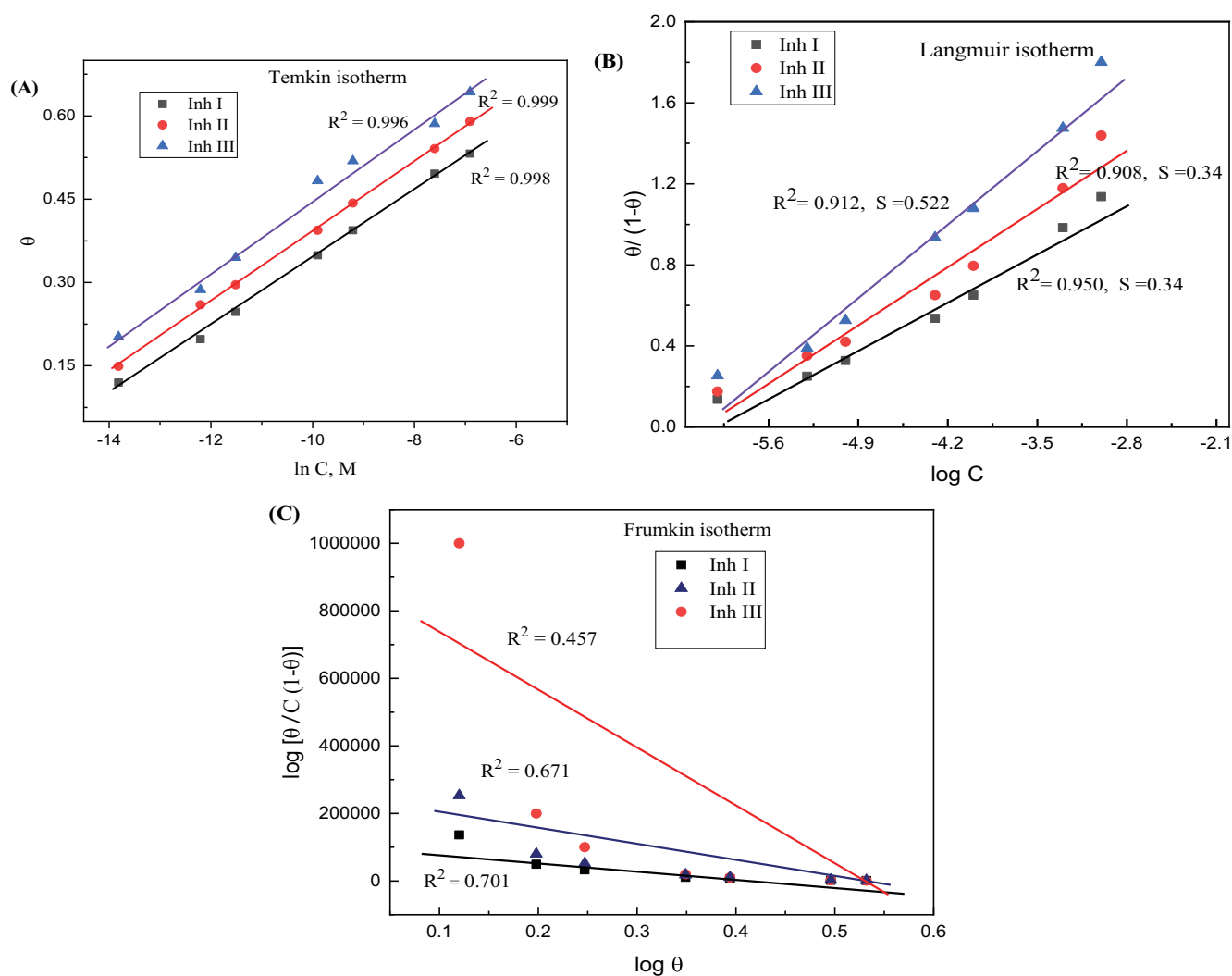| Type of anions	f	K_{ads}, mol	$-\Delta G°_{ads}$, KJ/mol
Inh I	16.31	6.027×10^6	48.63
Inh II	15.87	11.204×10^6	50.18
Inh III	15.41	22.056×10^6	51.84

Fig. 6. (A) Temkin, (B) Langmuir, and (C) Frumkin adsorption isotherm for various inhibitors on Ni in 0.01 M H_2SO_4 containing 0.01 M $NaClO_4$.

process including the transfer of electrons from the inhibitor molecules through the heteroatoms N, S, and π-electrons of the conjugated system of the benzene ring to the nickel-metal surface to form a coordinate bond [44].

3.3. Influence of temperature

The temperature plays a significant role in the investigation of the immutability of the inhibition processes. To evaluate the influence of temperature (range 25°C–50°C) experimentally, the Ni electrode is anodically polarized in 0.01 M H_2SO_4 containing 0.01 M ClO_4^- ions without and with 0.0001 M of various inhibitors. As expected, the value of E_p was found to shift in the more negative value due to the increase in the average kinetic energy of the corrosive species [45].

Fig. 7 depicts the polarization data of Ni in 0.01 M H_2SO_4 mixed with 0.01 M $NaClO_4$ devoid of and containing 0.0001 M of 3-allyl-1-[(2-methoxyphenyl)methyl]-thiourea. Similar curves are gained in the case of 0.0001 M of thiourea and N-allylthiourea (curves not displayed). Fig. 7 and the similar ones indicated that the rise in the solution temperature increases the time needed for the active oxidation of Ni metal and passive film formation with an enhancement of the pitting corrosion. It is noteworthy to see that the rate of oxide film formation (region III), $\partial E/\partial t$, is delayed with the displacement of E_{pit} into the more active values with raising the temperature. The increase in the induction time during Ni oxidation and the decrease in the rate of buildup of the Ni oxide layer by the temperature can be related to the probability of the increase in the mobility of ions by heating [46].

The quantity of electricity consumed during the passivation and before the initiation of pitting corrosion, Q, is increased with temperature as shown in Fig. 8. On the other hand, the change in $\partial E/\partial t$ is reduced by lowering in the slope of the potential-time curve (zone III) of Fig. 7. This attitude can be confirmed by Fig. 9 which depicts a straight-line relation between the log Q and the temperature, T for the free, and the inhibitive solutions.
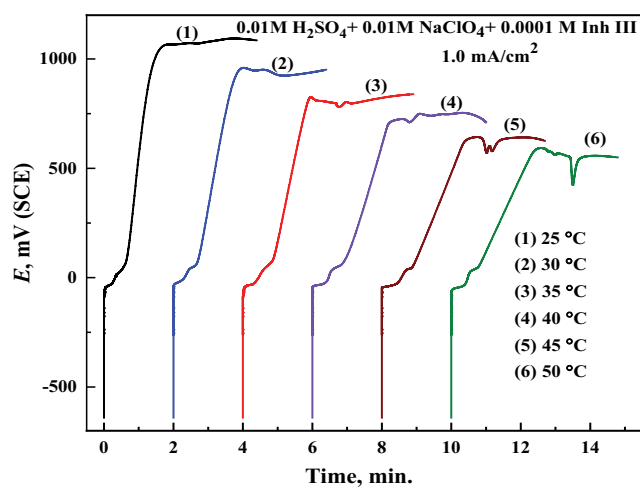
However, the Arrhenius equation can be utilized to compute the activation energy, E_a, for the damage of the oxide layer with the initiation of the pitting corrosion on the Ni surface using the following equation [25,47–50]:

$$\log r = \frac{-E_a^\circ}{2.303RT} + \log A \tag{6}$$

where r depicts the rate of corrosion reaction represented by the quantity of electricity (Q) required to reach E_{pit} and E_a is the apparent activation energy required for oxide film destruction, T is the absolute temperature, A is the Arrhenius constant, and R is the gas constant (8.314 J/K mol).

The values of log Q (in mC/cm^2 units), calculated at various temperatures are plotted against $1/T$, Fig. 10, in the case of 0.01 M H_2SO_4 mixed with 0.01 M $NaClO_4$ without and with 0.0001 M of various inhibitors. The activation
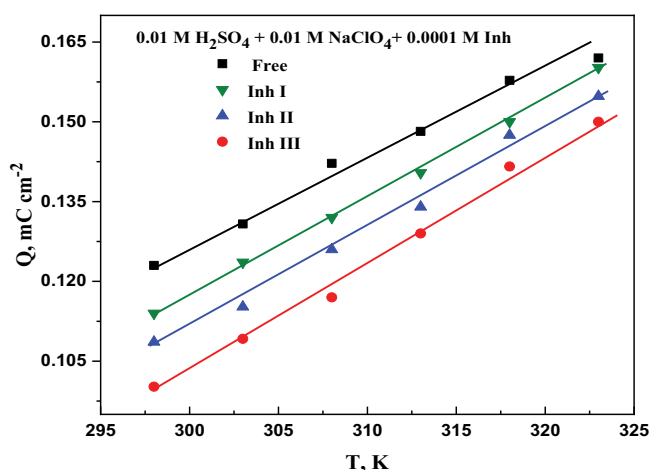
Fig. 8. Variation of the quantity of electricity, Q, with the temperature, T, for Ni in 0.01 M H_2SO_4 containing 0.01 M $NaClO_4$ and 0.0001 M inhibitors.

Fig. 7. Effect of temperature on the anodic polariziation curves of Ni in 0.01 M H_2SO_4 mixed with 0.01 M $NaClO_4$ and 1 × 10^{-4} M of 3-allyl-1-[(2-methoxyphenyl)methyl]thiourea.
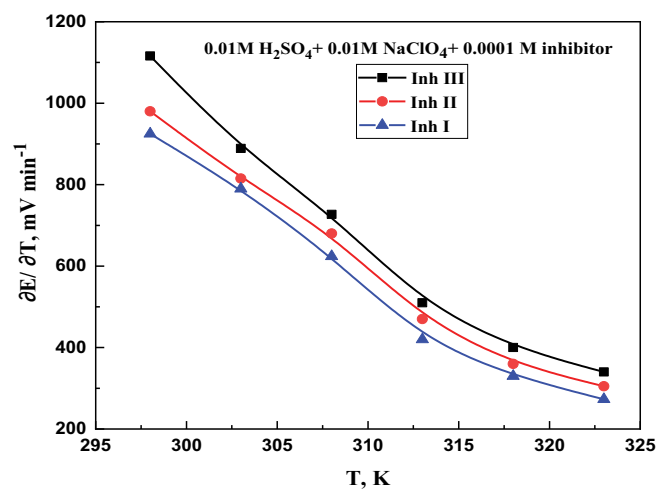
Fig. 9. Variation of the rate of oxide film repair, $(\partial E/\partial t)_{t'}$ with the temperature for Ni in 0.01 M H_2SO_4 containing 0.01 M $NaClO_4$ and 0.0001 M of various inhibitors.

energies, E_a were determined from the slope values and are listed in Table 4. The value of $E_{a'}$ for the pitting corrosion of Ni in 0.01 M H_2SO_4 and 0.01 M $NaClO_4$ was 9.39 kJ/mol [6]. The data of Table 4 shows the increase in
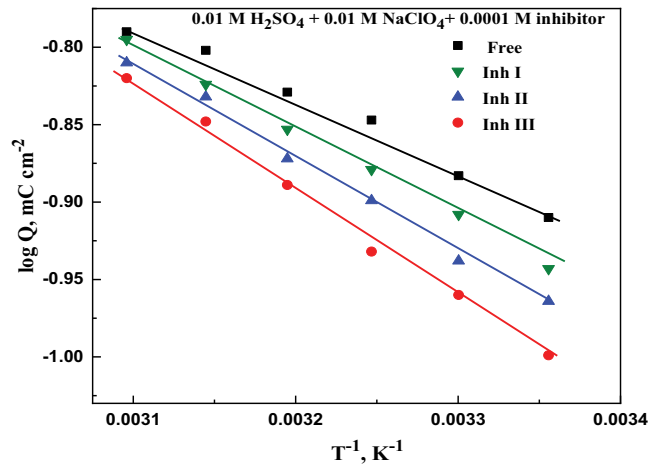

Fig. 10. Arrhenius plots for Ni in 0.01 M H_2SO_4 mixed with 0.01 M $NaClO_4$ in the absence and presence of 1×10^{-4} M of inhibitors.
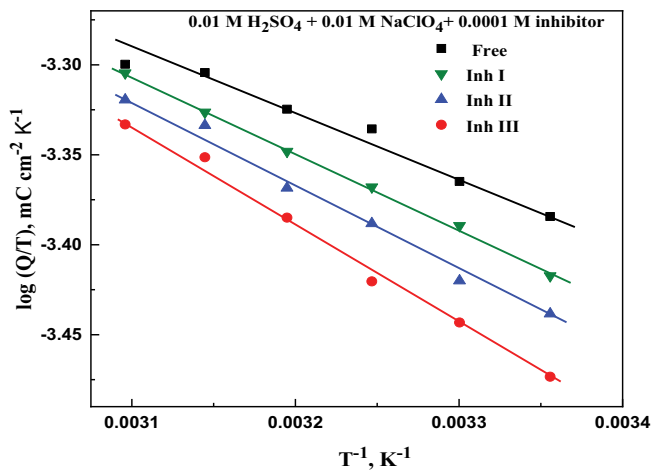

Fig. 11. Transition-state plots for Ni in 0.01 M H_2SO_4 mixed with 0.01 M $NaClO_4$ in the absence and presence of 1×10^{-4} M of inhibitors.

Table 4
Thermodynamic corrosion parameters, activation energy for pitting corrosion, E_a, enthalpy and entropy of Ni in 0.01 M H_2SO_4 mixed with 0.01 M $NaClO_4$ and 0.0001 M inhibitors

Type of anions	E_a, kJ/mol	ΔH, kJ/mol	$-\Delta S$, J/mol
0.01 M ClO_4^-	9.39	7.28	–238
0.01 M ClO_4^- + 0.0001 M Inh III	10.50	8.15	–235
0.01 M ClO_4^- + 0.0001 M Inh II	11.74	9.20	–232
0.01 M ClO_4^- + 0.0001 M Inh I	13.40	10.66	–228

E_a value when using inhibitors which are associated with the physical adsorption process. The more rise in the E_a value in the case of Inh III could be related to the high adsorption ability of such molecules sustaining passive film formation. Such attitude could be due related to the presence of more adsorption centers on 3-allyl-1-[(2-methoxyphenyl)methyl]thiourea which increases the energy barrier preventing the metal from the destructive effect of ClO_4^- and Cl^- ions.

According to the transition state equation [47–50]:

$$\log\left(\frac{r}{T}\right) = \log\left(\frac{R}{hN}\right) + \frac{\Delta S_a}{2.303R} - \frac{\Delta H_a}{2.303RT} \qquad (7)$$

where h and N are the Plank's and the Avogadro's number, respectively, while ΔS_a and ΔH_a are the enthalpies, and entropy of activation, respectively, of the destruction of the oxide film and initiation of pitting corrosion. This transition state equation is utilized to compute the thermodynamic activation parameters (ΔS_a and ΔH_a) accompanied by the activation process during the oxide film annihilation and initiation of pitting corrosion [46]. Fig. 11 represents the plots of $\log(r/T)$ against $1/T$ in case of the aggressive solution (0.01 M H_2SO_4 + 0.01 M $NaClO_3$) and the inhibitive solutions (0.01 M H_2SO_4 + 0.01 M $NaClO_3$ + 0.0001 M inhibitor). The data of this figure indicates straight-line relations representing the transition state plots. The values of ΔH_a and ΔS_a are determined from the values of the slopes, $-\Delta H_a/2.303R$ and the intercept, $\log(R/hN) + \Delta S_a/2.303R)$ and are listed in Table 4. The values of ΔH_a are varied between 8.15 and 10.66 kJ/mol and takes a positive sign which confirms the endothermic nature of the breakdown of passivity and initiation of the pitting corrosion on the Ni surface. The negative values of entropy, ΔS_a revealed a reduction in the disorder during the transformation of the reactants into an activated complex on the Ni metal surface [50].

4. Conclusion

The galvanostatic anodic polarization studies of Ni in 0.01 M H_2SO_4 containing 0.01 M $NaClO_4$ in the presence of different additions of thiourea, N-allylthiourea, and 3-allyl-1-[(2-methoxyphenyl)methyl]thiourea indicated that:

- ClO_4^- ions destruct the passive oxide film with several irregularly distributed pits on the Ni surface.
- The inhibitors increase the rate of oxide film formation, $\partial E/\partial t$, and shift E_{pit} into the noble direction.
- The retardation of pitting corrosion could be referred to the adsorption of the organic molecules through active centers on the Ni metal surface according to the Temkin model.
- 3-Allyl-1-[(2-methoxyphenyl)methyl]thiourea exhibits high inhibition performance due to the increase in the number of electron rich centers in the molecules.
- The temperature increases the initiation of pitting corrosion of Ni by enhancement of oxide film destruction by the ClO_4^- ions.
- The activation energy required to destruct the oxide film and initiate the pitting are increased with the additions

of inhibitors due to the formation of a barrier passive film.

Disclosure statement

The authors declare no potential conflict of interest in preparing this article.

References

[1] S. Abd El Wanees, A. El Aal, E.E. Abd El Aal, Anodic behavior and passivation of a lead electrode in sodium carbonate solutions, Br. Corros. J., 28 (1993) 222–226.

[2] S. Abd El Wanees, E.E. Abd El Aal, A. Abd El Aal, Inhibition of pitting corrosion of Pb in alkaline chlorate and perchlorate solutions by some inorganic anions, Anti-Corros. Methods Mater., 38 (1993) 4–8.

[3] S.M. Abd El Haleem, S. Abd El Wanees, E.E. Abd El Aal, A. Farouk, Factors affecting the corrosion behavior of aluminum in acid solutions. I. Nitrogen and/or sulphur-containing organic compounds as corrosion inhibitors for Al in HCl solutions, Corros. Sci., 68 (2013) 1–13.

[4] S.M. Abd El Haleem, S. Abd El Wanees, E.E. Abd El Aal, A. Diab, Environmental factors affecting the corrosion behavior of reinforcing steel II. Role of some anions in the initiation and inhibition of pitting corrosion of steel in $Ca(OH)_2$ solutions, Corros. Sci., 52 (2010) 292–302.

[5] S. Abd El Wanees, A.B. Radwan, M.A. Alsharif, S.M. Abd El Haleem, Initiation and inhibition of pitting corrosion on reinforcing steel under natural corrosion conditions, Mater. Chem. Phys., 190 (2017) 79–95.

[6] S. Abd El Wanees, A.S. Al-Gorair, H. Hawsawi, S.S. Elyan, M. Abdallah, Galvanostatic anodic polarization of Ni in sulfuric acid solution. II. Initiation and inhibition of pitting corrosion by some inorganic passivators, Int. J. Electrochem. Sci., 16 (2021) 1–14, 210548, doi: 10.20964/2021.05.25.

[7] G.T. Burstein, R.M. Souto, Observations of localized instability of passive titanium in chloride solution, Electrochim. Acta, 40 (1995) 1881–1888.

[8] H.S. Isaacs, The localized breakdown and repair of passive surfaces during pitting, Corros. Sci., 29 (1989) 313–323.

[9] P.C. Pistorius, G.T. Burstein, Metastable pitting corrosion of stainless steel and the transition to stability, Philos. Trans. R. Soc. London, Ser. A, 341 (1992) 531–559.

[10] S. Abd El Wanees, A. Abd El Aal, M. Abd El Azeem, A.N. Abd El Fatah, Pitting corrosion currents of tin in relation to the concentration of the inhibitive and corrosive anions under natural corrosion conditions, Int. J. Electrochem. Sci., 3 (2008) 1005–1015.

[11] E.E. Abd El Aal, S. Abd El Wanees, Galvanostatic study of the breakdown of Zn passivity by sulphate anions, Corros. Sci., 51 (2009) 1780–1788.

[12] M. Abdallah, I. Zaafarany, S. Abd El Wanees, R. Assi, Breakdown of passivity of nickel electrode in sulfuric acid and its inhibition by pyridinone derivatives using the galvanostatic polarization technique, Int. J. Corros. Scale Inhib., 4 (2015) 338–352.

[13] E.E. Abd El Aal, S. Abd El Wanees, A. Diab, S.M. Abd El Haleem, Environmental factors affecting the corrosion behavior of reinforcing steel III. Measurement of pitting corrosion currents of steel in $Ca(OH)_2$ solutions under natural corrosion conditions, Corros. Sci., 51 (2009) 1611–1618.

[14] M. Abdallah, S. Abd El Wanees, R. Assi, Effect of some analytical organic indicators on the corrosion of nickel in carbonate solution, Port. Electrochim. Acta, 27 (2009) 77–85.

[15] S. Abd El Wanees, M.I. Alahmdi, M. Abd El Azzem, H.E. Ahmed, 4, 6-Dimethyl-2-oxo-1, 2-dihydropyridine-3-carboxylic acid as an inhibitor towards the corrosion of C-steel in acetic acid, Int. J. Electrochem. Sci., 11 (2016) 3448–3466.

[16] S. Abd El Wanees, Amines as inhibitors for corrosion of copper in nitric acid, Anti-Corros. Methods Mater., 41 (1994) 3–7.

[17] S. Abd El Wanees, E.E. Abd El Aal, A. Abd El Aal, The inhibitive effect of some alcohols towards the corrosion of lead in nitric acid, Bull. Soc. Chim. Fr., 128 (1991) 889–893.

[18] S. Abd El Wanees, M.I. Alahmdi, M.A. Alsharif, Y. Atef, Mitigation of hydrogen evolution during zinc corrosion in aqueous acidic media using 5 Amino-4-imidazolecarboxamide, Egypt. J. Chem., 62 (2019) 811–825.

[19] S. Abd El Wanees, A.A.H. Bukhari, N.S. Alatawi, S. Salem, S. Nooh, S.K. Mustafa, Thermodynamic and adsorption studies on the corrosion inhibition of Zn by 2,2′-dithiobis- (2,3-dihydro-1,3-benzothiazole) in HCl solutions, Egypt. J. Chem., 64 (2021) 547–559.

[20] Z.A. Abdallah, M.S. Ahmed, M.M. Saleh, Organic synthesis and inhibition action of novel hydrazide derivative for mild steel corrosion in acid solutions, Mater. Chem Phys., 174 (2016) 91–99.

[21] S. Abd El Wanees, M. Abdallah, A.S. Al-Gorair, F.A.A. Tirkistani, S. Nooh, R. Assi, Investigation of anodic behavior of nickel in H_2SO_4 solutions using galvanostatic polarization technique. I. Kinetics and thermodynamic approach, Int. J. Electrochem. Sci., 16 (2021) 1–18, 150969, doi: 10.20964/2021.01.15.

[22] J.R. Kish, M.B. Ives, J.R. Rodda, Corrosion mechanism of Nickel in hot concentrated H_2SO_4, J. Electrochem. Soc., 147 (2000) 3637–3646.

[23] L.Z. Mohamed, Corrosion behavior of Ni and Ni-base alloy in acidic solutions, Egypt. J. Chem., 64 (2021) 133–142, doi: 10.21608/ejchem.2020.40019.2814.

[24] S.M. Abd El Haleem, S. Abd El Wanees, A. Bahgat, Environmental factors affecting the corrosion behaviour of reinforcing steel. V. Role of chloride and sulphate ions in the corrosion of reinforcing steel in saturated $Ca(OH)_2$ solutions, Corros. Sci., 75 (2013) 1–15.

[25] M.G.A. Saleh, S. Abd El Wanees, S. Khalid Mustafa, Dihydropyridine derivatives as controllers for production of hydrogen during zinc dissolution, Chem. Eng. Commun., 206 (2019) 789–803.

[26] S. Abd El Wanees S.H. Seda, Corrosion inhibition of zinc in aqueous acidic media using a novel synthesized Schiff Base–an experimental and theoretical study, J. Dispersion Sci. Technol., 40 (2019) 1813–1826.

[27] S. Abd El Wanees, E.E. Abd El Aal, N-Phenylcinnamimide and some of its derivatives as inhibitors for corrosion of lead in HCl solutions, Corros. Sci., 52 (2010) 338–344.

[28] F.M. Abd El Wahab, J.M. Abd El Kader, H.A. El Shayed, A.M. Shams El Din, On the pitting corrosion of tin in aqueous solutions, Corros. Sci., 18 (1978) 997–1009.

[29] E.E. Abd El Aal, S. Abd El Wanees, Kinetics of anodic behavior of Pb in HCl solutions, Corros. Sci., 51 (2009) 458–462.

[30] Y. Xie, T. Dinh, N. Jianqiang, Z. David, J. Young, Corrosion behavior of Ni-Cr alloys in wet CO_2 atmosphere at 700 and 800°C, Corros. Sci., 146 (2019) 28–43.

[31] B. Mac Dougal, D.F. Mitchell, M.J. Graham, Galvanostatic oxidation of nickel in borate buffer solution, J. Electrochem. Soc., 127 (1980) 1248–1253.

[32] M. Pourbaix, Atlas of Electrochemical Equilibria, Pergamon Press, Oxford, UK, 1996, 330 p.

[33] R. Nishimura, Pitting corrosion of nickel in borate and phosphate solutions, Corrosion, 43 (1987) 486–492.

[34] S.M. Abd El-Haleem, S. Abd El Wanees, Chloride induced pitting corrosion of nickel in alkaline solutions and its inhibition by organic amines, Mater. Chem. Phys., 128 (2011) 418–426.

[35] E.E. Abd El Aal, Breakdown of the passive film on nickel in borate solutions containing halide anions, Corros. Sci., 45 (2003) 759–775.

[36] M. Pagitsas, M. Pavlidou, D. Sazou, Localized passivity breakdown of iron in chlorate- and perchlorate-containing sulphuric acid solutions: a study based on current oscillations and a point defect model, Electrochim. Acta, 53 (2008) 4784–4795.

[37] D. Sazou, A. Kominia, M. Pagitsas, Corrosion processes of iron in acidic solutions associated with potential oscillations induced by chlorates and perchlorates, J. Solid State Electrochem., 18 (2014) 347–360.

[38] R. Nishimura, M. Araki, K. Kudo, Breakdown of passive film on iron, Corrosion, 40 (1984) 465–470.

[39] L. Niu, H. Zhang, F. Wie, S. Wu, X. Cao, P. Liu, Corrosion inhibition of iron in acidic solutions by alkyl quaternary ammonium halides: correlation between inhibition efficiency and molecular structure, Appl. Surf. Sci., 252 (2005) 1634–1642.

[40] S. Abd El Wanees, A.A. Mohamed, M. Abd El Azeem, R. El Said, Inhibition of silver corrosion in nitric acid by some aliphatic amines, J. Dispersion Sci. Technol., 31 (2009) 1516–1525.

[41] M. Hosseini, S.F.L. Mertens, M. Ghorbani, M.R. Arshadi, Asymmetrical Schiff bases as inhibitors of mild steel corrosion in sulphuric acid media, Mater. Chem. Phys., 78 (2003) 800–808.

[42] A. Yurt, G. Bereket, A. Kıvrak, A. Balaban, B. Erk, Effect of Schiff bases containing pyridyl group as corrosion inhibitors for low carbon steel in 0.1 M HCl, J. Appl. Electrochem., 35 (2005) 1025–1032.

[43] S.M. Abd El Haleem, S. Abd El Wanees, A. Bahgat, Environmental factors affecting the corrosion behavior of reinforcing steel. VI. Benzotriazole and its derivatives as corrosion inhibitors of steel, Corros. Sci., 87 (2014) 321–333.

[44] E.E. Abd El Aal, Breakdown of passive film on nickel in borate solutions containing halide anions, Corros. Sci., 45 (2003) 759–775.

[45] W. Zhang, B. Nie, H.-J. Li, Q. Li, C. Li, Y.-C. Wu, Inhibition of mild steel corrosion in 1 M HCl by chondroitin sulfate and its synergistic effect with sodium alginate, Carbohydr. Polym., 260 (2021) 1–10, 117842, doi: 10.1016/j.carbpol.2021.117842.

[46] A. Attou, M. Tourabi, A. Benikdes, O. Benali, H.B. Quici, F. Benhiba, A. Zarrouke, C. Jama, F. Bentiss, Experimental studies and computational exploration on the 2-amino-5-(2-methoxyphenyl)-1,3,4-thiadiazole as novel corrosion inhibitor for mild steel in acidic environment, Colloids Surf., A, 604 (2020) 1–18, 125320, doi: 10.1016/j.colsurfa.2020.125320.

[47] M. Abdallah, H.M. Altass, A.S. Al-Gorair, J.H. Al-Fahemi, K.A. Soliman, Natural nutmeg oil as a green corrosion inhibitor for carbon steel in 1.0 M HCl solution: chemical, electrochemical, and computational methods, J. Mol. Liq., 323 (2021) 1–12, 115036, doi: 10.1016/j.molliq.2020.115036.

[48] S. Abd El Wanees, M.I. Alahmdi, S.M. Rashwan, M.M. Kamel, M.G. Abd Elsadek, Inhibitive effect of cetyltriphenylphosphonium bromide on C-steel corrosion in HCl solution, Int. J. Electrochem. Sci., 11 (2016) 9265–9281.

[49] S. Abd El Wanees, A. Diab, O. Azazy, M.A. El Azim, Inhibition effect of N-(pyridin-2-yl-carbamothioyl)benzamide on the corrosion of C-steel in sulfuric acid solutions, J. Dispersion Sci. Technol., 35 (2014) 1571–1580.

[50] M. Yadav S. Kumar, N. Tiwari, I. Bahadur, E.E. Ebenso, Experimental and quantum chemical studies of synthesized triazine derivatives as an efficient corrosion inhibitor for N80 steel in acidic medium, J. Mol. Liq., 212 (2015) 151–167.